Research Article

Journal of RAMAN SPECTROSCOPY

Received: 1 May 2009 Accepted: 3 August 2009 Published online in Wiley Interscience: 21 September 2009

(www.interscience.wiley.com) DOI 10.1002/jrs.2474

Destruction of the short-range disorder due to erbium doping in $Pb_{0.8}La_{0.2}TiO_3$ films

Tung-Ching Huang and Wen-Feng Hsieh*

We show the destruction of a displacement of Ti in the short-range structure by observing the disappearance of emission and Raman signals when the Er^{3+} concentration exceeds 7 mol% in sol–gel-derived $Pb_{0.8}La_{0.2}TiO_3$ polycrystalline films. It is believed that there always exists disorder due to displacement of B ions in the skeleton of BO_6 in perovskite ABO_3 materials. This disorder due to the displacement of Ti ions breaks the center of symmetry to activate emission of rare-earth ions such as Er^{3+} and Raman modes of perovskites. We found that the breaking of symmetry can be diminished by introducing more Er^{3+} ions. Copyright © 2009 John Wiley & Sons, Ltd.

Keywords: X-ray diffraction; crystal structure; rare earth; lattice dynamics; emission

Introduction

Rare-earth ions exhibit characteristics of intra-4f shell electrons which emit light from visible to infrared wavelengths, which have potential applications in photonic devices.[1–3] Erbium-doped materials have been particularly investigated because of the blue ($^2H_{9/2} \rightarrow {}^4I_{15/2}$), green ($^4S_{3/2}, ^2H_{11/2} \rightarrow {}^4I_{15/2}$), red ($^4F_{9/2} \rightarrow {}^4I_{15/2}$), and infrared ($^4I_{13/2} \rightarrow {}^4I_{15/2}$) emission, and the emission has been realized in a variety of glasses and ferroelectric materials.[4–8] In comparison with glasses, ferroelectric materials such as barium strontium titanate ($Ba_{1-x}Sr_xTiO_3$) (BST) have the merits of better crystallinity and non-centrosymmetry to support high luminescence and excellent dielectric properties, such as high dielectric constant, small dielectric loss, low leakage current, and large dielectric breakdown strength[9] in the microwave frequency range, that have application for electronic circuits, and should be potentially applicable in an optoelectronic integrated system with Er^{3+} doping for making light emitting devices.

Dobal *et al.*[10] and Bhaskar *et al.*[11] reported that the structure of the sol–gel-derived $Pb_{1-x}La_xTiO_3$ polycrystalline films on (0001) sapphire belongs to the cubic class for $x > 0.15$ from X-ray diffraction (XRD), whereas the Raman modes still could be observed even up to $x = 0.25$. They considered that the phonon modes exist above the transition temperature of the tetragonal-to-cubic phase transition in these solid solutions because of a displacement of Ti in the short-range structure in the paraelectric cubic phase.[10–12]

The erbium ions usually take the trivalent charge state when they are incorporated as an impurity into a dielectric host material and therefore make $Pb_{1-x}La_xTiO_3$ a better candidate for an erbium-doped host material over BST because they have the same ion valence as the lanthanum ion. One would expect a higher solubility, and hence a better emission efficiency, for erbium-doped $Pb_{1-x}La_xTiO_3$ film than for BST at room temperature (RT). However, the emission efficiency depends on not only the Er^{3+} concentration but also the probability of transitions among the levels in Er^{3+} ions. Furthermore, the sol–gel-derived $Pb_{1-x}La_xTiO_3$ films have high optical transparency in the visible region, and they have the best crystallinity[13] at $x = 0.2$.

We show in this paper, for the first time to our knowledge, a disappearance of emission and Raman signals in sol–gel-derived $Pb_{0.8}La_{0.2}TiO_3$ (PLT) films as a result of destruction of the displacement of Ti in the short-range structure but keeping the perovskite phase when the Er^{3+} concentration exceeds 7 mol%.

Experimental

Er^{3+}-doped PLT polycrystalline films were grown on $Pt/Ti/SiO_2/Si$ substrates by the sol–gel method. The starting materials were high-purity lead acetate, lanthanum acetate, titanium isopropoxide, and erbium acetate. Lead acetate and lanthanum acetate in the molar ratios of 8 : 2 and an appropriate mole of erbium acetate were dissolved in 2-methoxyethanol and stirred for 10 min at 110 °C to remove the associated water of crystallization. The stoichiometric amount of titanium isopropoxide was then added to the sol at 80 °C while stirring continuously for approximately 10 min. The diluted solution was then spin-coated on clean $Pt/Ti/SiO_2/Si$ substrates, which had been previously cleaned thoroughly in a series of organic solvents in an ultrasonic cleaner. The coated films were heated at 200 °C in ambient atmosphere for 10 min to dry the gel. To increase the film thickness, we coated the samples by the aforementioned process ten times, which corresponds to a thickness of about 800 nm as determined by scanning electron microscopy (SEM) of the cross section. Finally, the samples were sintered in a furnace at various temperatures between 650 and 1100 °C for 1 h.

The XRD data of the films and powders were measured using a Mac science M18X X-ray diffractometer equipped with a rotating anode (Cu Kα line of 1.5405 Å). The visible emission and Raman spectral measurements were collected by a SPEX 1877C triple

* *Correspondence to: Wen-Feng Hsieh, Department of Photonics and Institute of Electro-Optical Engineering, National Chiao Tung University, 1001 Tahsueh Rd., Hsinchu 30050, Taiwan. E-mail: wfhsieh@mail.nctu.edu.tw*

Department of Photonics and Institute of Electro-Optical Engineering, National Chiao Tung University, Hsinchu 30050, Taiwan

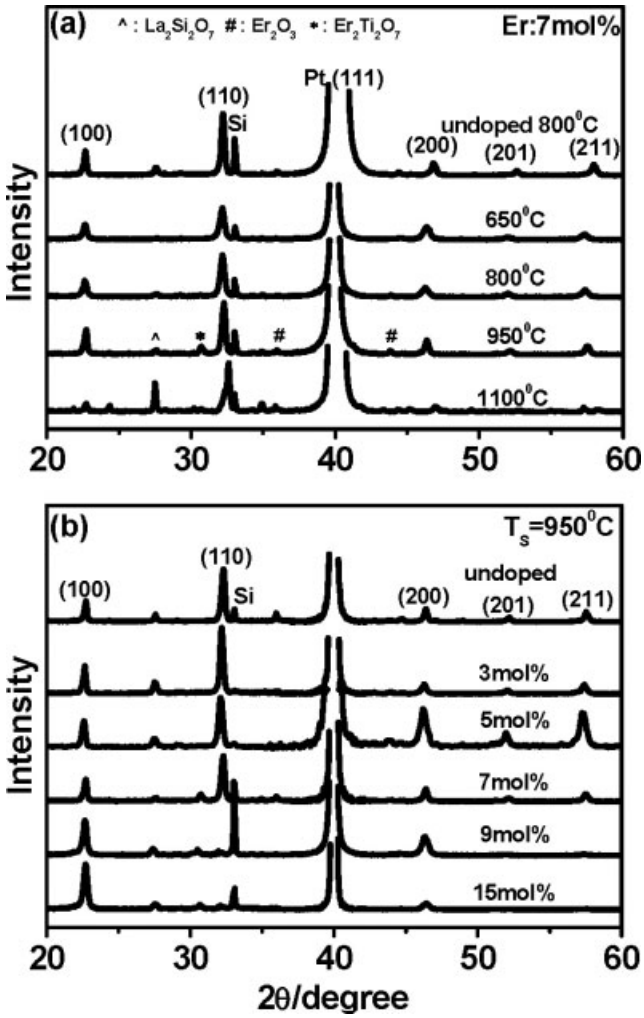

Figure 1. XRD patterns of Er^{3+}-doped PLT films with 7 mol% Er^{3+} doping at various sintering temperatures (a) and with different Er^{3+} concentrations at a sintering temperature of 950 °C (b).

spectrograph equipped with a liquid-nitrogen-cooled charge-coupled device at 140 K under the excitation of an argon ion laser line at 488 nm wavelength, while the IR emission spectroscopy was performed using a Jobin Yvon HR-1000 monochromator with an InGaAs detector. The excitation source was the 488-nm line of an argon ion laser with power of 40 mW on the tested films.

Results and Discussion

Figure 1(a) shows the XRD patterns of 7 mol% Er^{3+}-doped PLT films on Pt/Ti/SiO_2/Si substrates at various sintering temperatures between 650 and 1100 °C; the pattern of undoped PLT film at 800 °C is also shown for comparison. The Er^{3+}-doped PLT film sintered at 650 °C shows a perovskite phase with (100), (110), (200), (210), and (211) planes without obvious secondary phases. As the films are sintered at 800 and 950 °C, the diffraction peaks of the perovskite phase become more intense and their full widths at half-maximum (FWHMs) become smaller. It indicates that the films have better crystallinity at the higher sintering temperatures even though weak secondary phases appear. We found small signatures of the secondary $Er_2Ti_2O_7$ phase appearing at 31° and Er_2O_3 phase at 36° and 43.7° for sintering at 950 °C. By further raising the

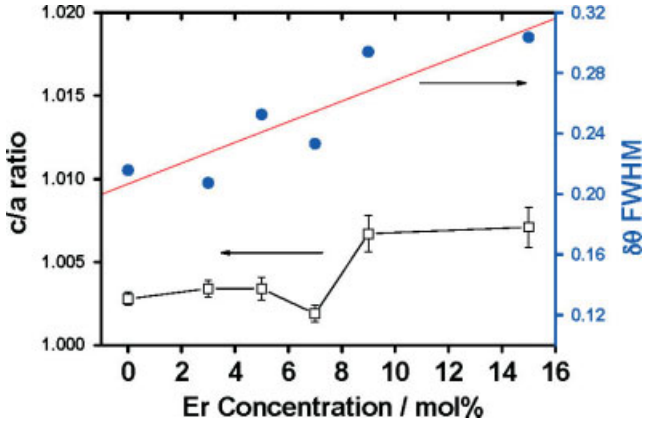

Figure 2. The ratio of lattice constants *c*/*a* after Rietvelt refinement and the FWHM of (100) with different Er^{3+} concentrations at a sintering temperature 950 °C.

sintering temperature to 1100 °C, the strong peaks at 27° due to $La_2Si_2O_7$ consistent with the Joint Committee on Powder Diffraction Standards (JCPDS) data were recognized. It is believed that the $La_2Si_2O_7$ phase appeared at the interface between Er^{3+}-doped PLT thin films and the silicon substrate during the process of the high-temperature sintering. And, the peaks of the perovskite phase become weaker, or even vanish, indicating the destruction of the perovskite structure. The FWHMs of (100) peaks analyzed from the result of XRD pattern in Fig. 1(a) tend to decrease from 0.28° to 0.22°, corresponding to the crystal diameter ranging from 28.9 to 36.8 nm, while increasing the sintering temperature from 650 to 950 °C. The better crystallinity for the higher sintering temperature is universally known.

Figure 1(b) shows the XRD patterns of PLT films on Pt/Ti/SiO_2/Si doped with different Er^{3+} concentrations after being sintered at 950 °C. All the films possess even better perovskite crystallinity, although several weak secondary phases appear. As expected, due to the same charge state, Er^{3+} may take the positions of La^{3+} in the lattice. It indicates that Er^{3+} dissolved in PLT takes over 15 mol% without destroying the crystallinity in the PLT system, which exceeds the result of the BST system[8] of 3 mol%. Although the XRD intensity of (110) and (211) planes is slightly different for 9 and 15 mol% Er^{3+}-doped samples, which may be not ascribed to alignments, the results still confirmed a good pervoskite phase in these Er^{3+}-doped PLT powders.

In order to investigate the variation of long-range structures with the increase of Er^{3+} concentration, the XRD patterns in Fig. 1(b) were further analyzed with a refinement procedure. We used the tetragonal structure for all samples to obtain the ratio of lattice constants *c*/*a*. The initial data of (100), (110), (200), (201), and (211) planes identified with the JCPDS data are input to the XLAT program.[14] Plotted in Fig. 2 are the FWHM of (100) and *c*/*a versus* the Er^{3+} concentration. The FWHM tends to linearly increase from 0.22° to 0.31°, corresponding to the crystal diameter ranging from 36.8 to 26.1 nm, as Er^{3+} doping increases from 0 to 15 mol%. It reveals a degradation of the crystallinity for the higher Er^{3+} doping. On the other hand, the ratio *c*/*a* is between 1.001 and 1.007, which is much smaller than that of $PbTiO_3$ (1.067) but comparable to or slightly larger than that[15] of $BaTiO_3$ (1.002). This indicates that the Er^{3+}-doped PLT films with different Er^{3+} concentrations of 0, 3, 5, 7, 9, and 15 mol%, all belong to the tetragonal phase. We found that *c*/*a* is around 1.002 for the undoped sample, slightly increases and then decreases to around 1.001 at 7 mol%, and

Journal of RAMAN SPECTROSCOPY

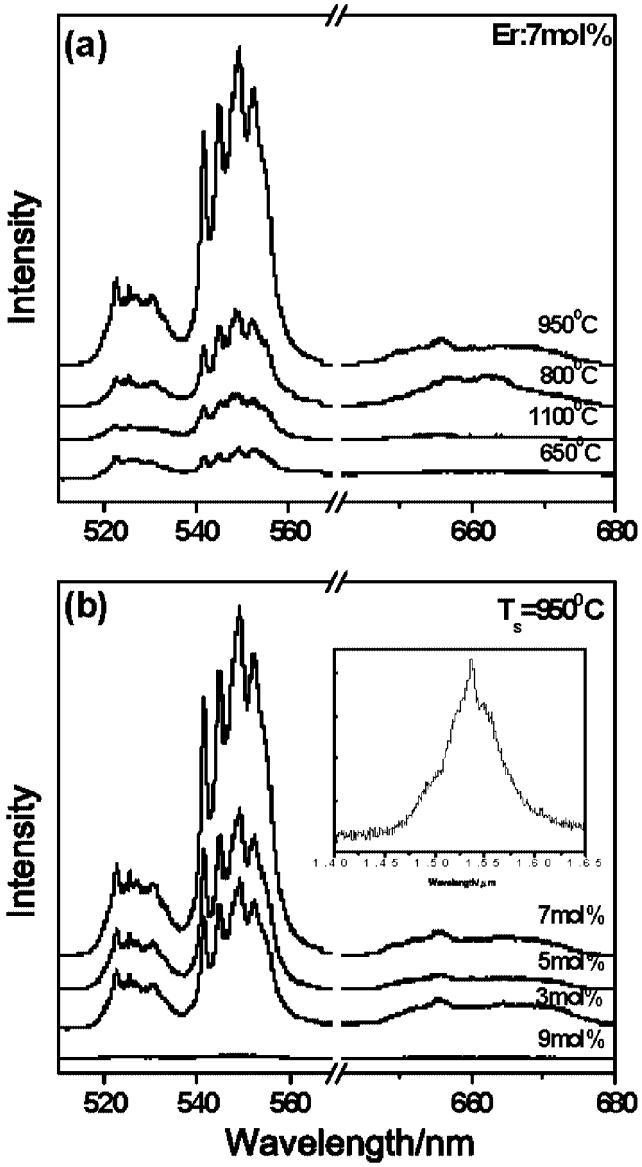

Figure 3. Dependence of the green emission intensities of Er^{3+}-doped PLT films on Er^{3+} concentrations and sintering temperature.

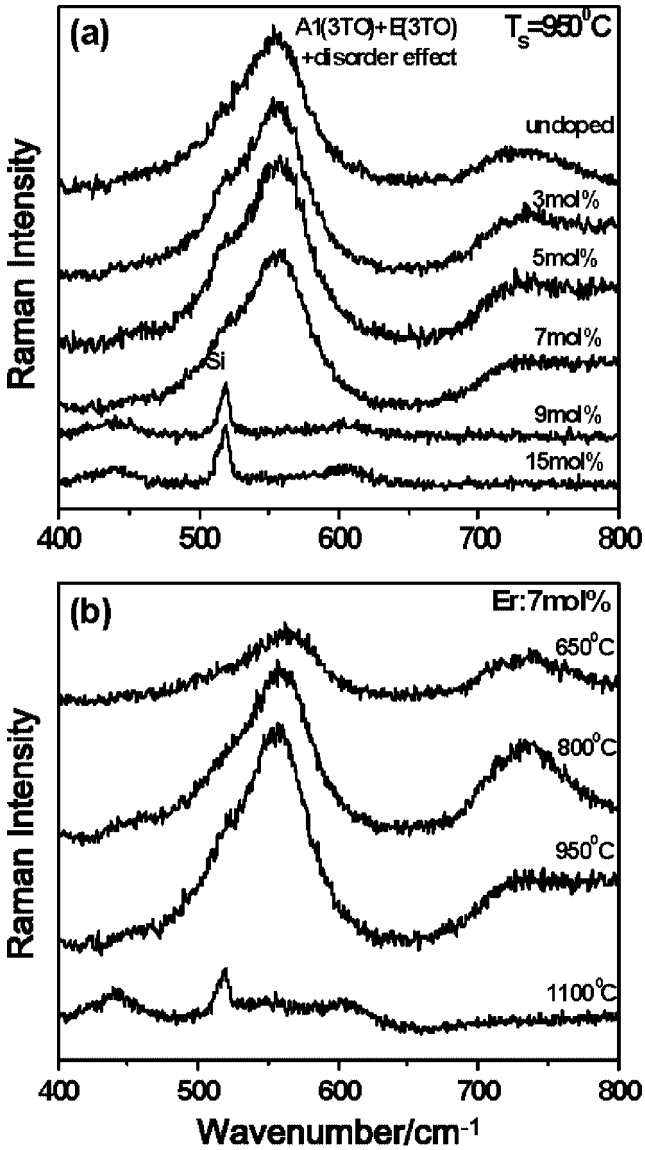

Figure 4. Raman spectra of Er^{3+}-doped PLT films with different Er^{3+} concentrations at a sintering temperature 950 °C (a) and with 7 mol% Er^{3+} doping at various sintering temperatures (b).

then increases to 1.007 for the samples with 9 and 15 mol%. The trend of *c*/*a* ratio with Er^{3+} concentration is similar to those reported by Dobal *et al*.[16] They reported that the tetragonality ratio *c*/*a* increases with increasing Gd content in rare-earth-doped $Pb_{0.90}La_{0.15}TiO_3$ thin films. As the Er^{3+} ion concentration increases or the host material possesses a higher tetragonality, we expected that a stronger emission would be observed. However, as we will show shortly, the maximum emission was observed at 7 mol% but no emission for Er^{3+} doping larger than 9 mol%, which possesses higher tetragonality (non-centrosymmetry) than the 7 mol% case.

Figure 3(a) shows the RT visible emission spectra of PLT films doped with 7 mol% Er^{3+} ions at sintering temperatures of 650, 800, 950, and 1100 °C. All the visible emission spectra have similar shapes, but they possess different emission behaviors. The strong green emission peaks at 530 and 550 nm are attributed to the Er^{3+} 4f–4f inner-shell transitions of $^2H_{11/2} \rightarrow {}^4I_{15/2}$ and $^4S_{3/2} \rightarrow {}^4I_{15/2}$, while the weak red emission centered at 660 nm is ascribed to $^4F_{9/2} \rightarrow {}^4I_{15/2}$. The splitting of the emission peaks is attributed to the Stark splitting of the degenerate 4f levels under the crystalline field of the host material. As expected, the better the crystallinity (see Fig. 1(a)), the higher the emission on increasing the sintering temperature from 650 to 950 °C, and the weaker the emission at 1100 °C sintering.

The high Er^{3+} concentration also might mean the high emission efficiency, and Fig. 3(b) displays the spectra of PLT films doped with different Er^{3+} concentrations of 3, 5, 7, and 9 mol% after sintering at 950 °C. However, the emission intensity of the Er^{3+}-doped PLT films does increase as the activated Er^{3+} doping increases until 7 mol%, but quickly decreases as the Er^{3+}-doping concentration exceeds 7 mol%. The quenching mechanism was thought to be a cross-relaxation process between two closely placed Er^{3+} ions.[17–19]

In this study, the ion density *N* of 3, 5, 7, and 9 mol% Er^{3+} doping is about 4.9×10^{20}, 8.2×10^{20}, 11.4×10^{20}, and $14.7 \times 10^{20}/cm^3$, respectively, and the mean distance[20] among

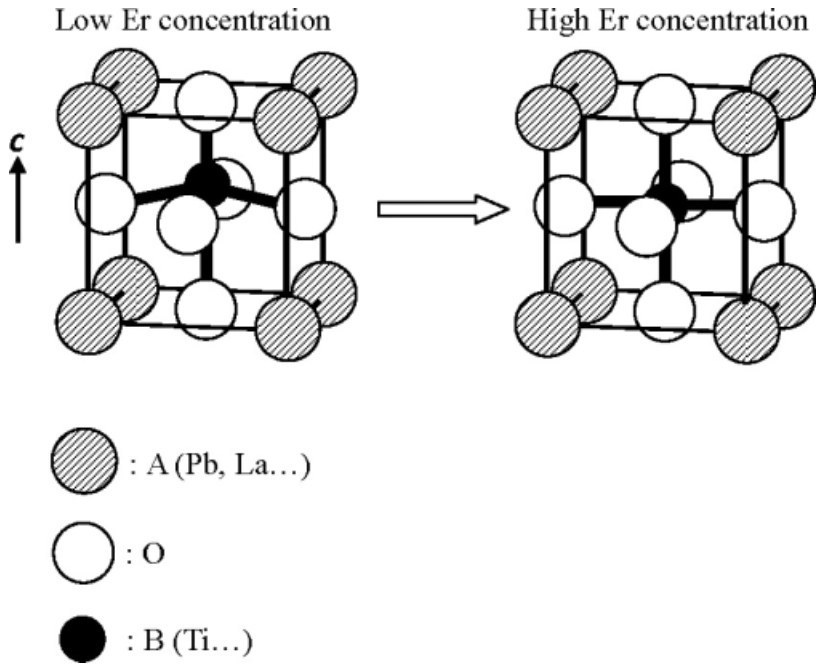

Figure 5. Schematic representation of the position of B atom in ABO_3 structure.

Er^{3+} ions estimated by $\gamma = 0.62 \times N^{-1/3}$ is 7.8, 6.6, 5.9, and 5.5Å, correspondingly. The mean distance varies slowly with increasing Er^{3+} concentration from 7 to 9 mol%, while the emission efficiency decreases sharply. This indicates that the quenching mechanism might not be dominated by a cross-relaxation process, and there may be other dominant factors responsible for decreasing the emission efficiency in the Er^{3+}-doped PLT system. Looking at the result of Fig. 2, because the 9 mol% Er^{3+}-doped films do possess higher tetragonality (non-centrosymmetry) than the 7 mol% ones, the quenching mechanism also would not be dominated by the long-range structure and crystallinity. As proposed by Tanabe *et al.*,[21] the emission efficiency has to do with the degree of local structure symmetry and the quenching behavior is related to the local structure symmetry, which will be discussed with the results of the Raman measurement later on. In addition, we also observed the RT IR emission spectra of PLT films doped with 5 mol% Er^{3+} concentrations at 950 °C sintering (inset of Fig. 3(b)) under excitation with the 488 nm.

Figure 4(a) shows the Raman spectra of samples with different Er^{3+} concentrations in PLT sintered at 950 °C. Besides the weak, broad feature between 700 and 800 cm^{-1}, we found another broad band centered around 560 cm^{-1} which is attributed to $A_1(3TO) + E(3TO)$ phonon modes due to the reduced size of polycrystalline and the localized disorder of displacement of Ti ion from the center of the BO_6 skeleton.[17–19] These peaks remain almost unchanged as Er^{3+} concentration increases from 3 to 7 mol%, but vanish for samples with 9 and 15 mol% Er^{3+} concentrations; only Si LO phonon at 520 cm^{-1} from the Si substrate and phonon modes of amorphous native oxide around 440 and 600 cm^{-1} remain. The disappearance of Raman modes due to either a weak ferroelectric phase or a weak disorder effect (resulting from a displacement of Ti) is caused by a decrease in the crystal diameter which results in the formation of a centrosymmetric structure[22] with increasing Er^{3+} concentration. By comparing with the results of XRD, we found that a weakening of the disorder may be the dominant mechanism. In Fig. 5 is a schematic representation of the mechanism illustrating that Ti atom displaces off its central position and moves toward one oxygen as the Er^{3+} concentration is below or at 7 mol%. Nevertheless, it will return to its central position when the Er^{3+} concentration reaches or exceeds 9 mol%. Figure 4(b) shows the change of the Raman spectra of Er^{3+}-doped PLT films at 7 mol% Er^{3+} ions, with increasing annealing temperature from 650 to 1100 °C. We found a similar disappearance of these specific phonons resulting from conversion to a perovskite structure at sintering temperatures beyond 1100 °C.

It is interesting to correlate the Raman spectra of Fig. 4 with the green emission of Fig. 3. We found no variation in the ferroelectric and disorder modes from the Raman spectra, whereas the emission intensity of the Er^{3+}-doped PLT films increased as the Er^{3+} doping increased from 3 to 7 mol%. In contrast, by increasing the Er^{3+} concentration to 9 mol%, we found that the green emission and the disorder effect on Raman scattering suddenly diminished, indicating that the selection rule is strongly reinforced to eliminate the short-range disorder, and the crystal structure becomes strictly centrosymmetric.

Looking back at Figs 3(b) and 4(a), we find that the green emission becomes weaker and the disorder effect vanishes separately, but the crystal structure remains unchanged while increasing the Er^{3+} concentration to above 9 mol%. It reveals that the destruction of short-range disorder leads to lower efficiency of emission even though these films still possess good crystallinity. Thus, the symmetry over short range of the Er^{3+}-doped PLT crystal seems to influence the activity of Er^{3+} ions. A more symmetric structure of the host materials would reduce the transition probability within the 4f-inner shell of the Er^{3+} ion.[20]

Comparing the analyses of the emission and Raman spectra, the films possess a good perovskite phase at sintering temperatures of 600, 800, and 950 °C, so that they have similar visible emission spectral shapes and phonon modes. The weak perovskite phase at a sintering temperature of 650 °C results in weak emission, as strong emission originates from the best crystalline phase at

950 °C sintering. The unobvious split with relative low emission at 1100 °C sintering is due to the destruction of the structure.

Conclusion

Er^{3+}-doped $Pb_{0.8}La_{0.2}TiO_3$ films with perovskite structure were made on Pt/Ti/SiO_2/Si substrates by the sol–gel method. The dependence of emission efficiency on Er^{3+} concentration and sintering temperature is dominated by solubility and symmetry of the crystal structure. We have shown that destruction of the short-range disorder due to displacement of B ions exists in the skeleton of BO_6, as inferred from the disappearance of emission and Raman signals when the Er^{3+} concentration exceeded 7 mol%, although the samples still possess good long-range structure as confirmed by XRD. The crystal field due to the disorder effect that contributes to the perturbation term for the Er^{3+} 4f–4f inner-shell transitions is diminished when introducing more Er^{3+} ions.

Acknowledgements

This work is partially supported by the National Science Council of Taiwan under grants NSC-96-2628-M-009-001-MY3 and NSC-95-2221-E-133-001.

References

[1] E. Desurvire, *Erbium-Doped Fiber Amplifiers*, Wiley: New York, **1994**.
[2] B. Yan, X. Q. Su, *Opt. Mater.* **2007**, *29*, 547.
[3] J. Y. Allain, M. Monerie, H. Poignant, T. Georges, *J. Non-Cryst. Solids* **1993**, *161*, 270.
[4] J. Heikenfeld, M. Garter, D. S. Lee, R. Birkhahn, A. J. Steckl, *Appl. Phys. Lett.* **1999**, *75*, 1189.
[5] H. X. Zhang, C. H. Kam, Y. Zhou, X. Q. Han, S. Buddhudu, Q. Xiang, Y. L. Lam, Y. C. Chan, *Appl. Phys. Lett.* **2000**, *77*, 609.
[6] S. M. Takahashi, M. Kanno, R. Kawamoto, *Appl. Phys. Lett.* **1994**, *65*, 1874.
[7] J. Heikenfeld, D. S. Lee, M. Garter, R. Birkhahn, A. J. Steckl, *Appl. Phys. Lett.* **2000**, *76*, 1365.
[8] S. Y. Kuo, C. S. Chen, T. Y. Tseng, S. C. Chang, W. F. Hsieh, *J. Appl. Phys.* **2002**, *92*, 1868.
[9] H. C. Kang, S. Park, K. Kim, M. Y. Sung, H. Chai, *Electrochem. Solid-state Lett.* **2004**, *7*, F77.
[10] P. S. Dobal, S. B. Majumder, S. Bhaskar, R. S. Katiyar, *J. Raman Spectrosc.* **1999**, *30*, 567.
[11] S. Bhaskar, S. B. Majumder, R. S. Katiyar, *Appl. Phys. Lett.* **2002**, *80*, 3997.
[12] P. P. Neves, A. C. Doriguetto, V. R. Mastelaro, L. P. Lopes, Y. P. Mascarenhas, A. Michalowicz, J. A. Eiras, *J. Chem. Phys.* **2004**, *180*, 14840.
[13] S. B. Majumder, M. Jain, R. S. Katiyar, *Thin Solid Films* **2002**, *402*, 90.
[14] B. Rupp, A computer program for Rietveld analysis of x-ray and neutron powder diffraction patterns, http://www.ruppweb.org/weblat/weblat.htm, **2005**.
[15] S. Y. Kuo, W. Y. Liao, W. F. Hsieh, *Phys. Rev. B* **2001**, *64*, 224103.
[16] P. S. Dobal, R. R. Das, B. Roy, R. S. Katiyar, S. Jain, D. C. Agrawal, *J. Raman Spectrosc.* **2000**, *31*, 965.
[17] M. Fujii, M. Yoshida, S. Hayashi, K. Yamamoto, *J. Appl. Phys.* **1998**, *84*, 4525.
[18] T. M. Kozhan, V. V. Kusnetsova, P. R. Pershukevich, I. I. Serqeev V. S. Khomenko, *Spectrochim. Acta, Part A* **1999**, *55*, 1407.
[19] X. Chen, T. Nguyen, Q. Luu, B. DiBartolo, *J. Lumin.* **2000**, *85*, 295.
[20] C. Y. Chen, R. R. Petrin, D. C. Yeh, W. A. Sibley, J. L. Adam, *Opt. Lett.* **1989**, *14*, 432.
[21] S. Tanabe, T. Ohyagi, N. Soga, T. Hanada, *Phys. Rev. B* **1992**, *46*, 3305.
[22] V. Petkov, M. Gateshki, M. Niederberger, Y. Ren, *Chem. Mater.* **2006**, *18*, 814.